International Journal of Agriculture and Biosciences 2026 15(3): 974-983.
https://doi.org/10.47278/journal.ijab/2026.014

RESEARCH ARTICLE
eISSN: 2306-3599; pISSN: 2305-6622

A Novel Anti-MDR Activity and In Silico Pharmacological Profiling of 2,4-Di-tert-Butylphenol from Indonesian Peat Soil *Lysinibacillus* sp. against DNA Gyrase

Dede Mahdiyah [1]*, Bayu Hari Mukti [2], Putri Vidiasari Darsono [1] and Dwi Sogi Sri Redjeki [3]

[1]Department of Pharmacy, Faculty of Health, Universitas Sari Mulia, Banjarmasin, IndonesiaSari Mulia University, Indonesia
[2]Department of Industrial Engineering, Sari Mulia University, Indonesia
[3]Department of English Education, Sari Mulia University, Indonesia
*Corresponding author: mahdiyahmukti@gmail.com

ABSTRACT

The escalating global antimicrobial resistance (AMR) crisis drives the search for novel antibacterial compounds from underexplored sources. This study aimed to evaluate the broad-spectrum and anti-multi-drug resistant (MDR) activity of a *Lysinibacillus* isolate from Indonesian peat soil, identify its bioactive compound, and perform an in silico pharmacological profiling. Methods included antibacterial activity testing using the Kirby-Bauer disc diffusion assay against MDR and non-MDR pathogens, compound identification via Gas Chromatography-Mass Spectrometry (GC-MS), and prediction of ADMET properties, drug-likeness, and molecular docking simulations against DNA gyrase subunit B using various in silico platforms. Results demonstrated that the *Lysinibacillus* sp. supernatant exhibited broad inhibitory activity, including against MRSA (inhibition zone of 16.16mm) and ESBL-producing *E. coli* (11.76mm). GC-MS analysis identified 2,4-Di-tert-butylphenol (2,4-DTBP) as the primary compound. In silico profiling revealed that 2,4-DTBP complied with all Lipinski's rules, possessed low toxicity (LD_{50} 700mg/kg), a favourable pharmacokinetic profile (92% intestinal absorption, no inhibition of CYP450 enzymes), and strong binding affinity to DNA gyrase (-5.9kcal/mol). In conclusion, 2,4-DTBP from *Lysinibacillus* sp. is a promising antibacterial candidate, with a predicted mechanism of action via DNA gyrase inhibition, supported by an excellent in silico pharmacological profile for further development.

Keywords: *Lysinibacillus*, Antimicrobial resistance, 2,4-Di-tert-butylphenol, ADMET, GC-MS, DNA gyrase.

Article History
Article # 25-535
Received: 09-Sep-25
Revised: 05-Dec-25
Accepted: 25-Dec-25
Online First: 09-Jan-26

INTRODUCTION

The escalating crisis of antimicrobial resistance (AMR) represents one of the most formidable challenges to global health in the 21st century. A new World Health Organization (WHO) report, drawing on data from over 23 million confirmed infections across 110 countries (WHO, 2025). The persistent emergence and spread of Multi-Drug Resistant (MDR) pathogens, particularly the ESKAPE organisms (*Enterococcus faecium, Staphylococcus aureus, Klebsiella pneumoniae, Acinetobacter baumannii, Pseudomonas aeroginosa* and *Enterobacter* species), have severely eroded the efficacy of existing antibiotic arsenals. Pathogens have developed diverse resistance mechanisms, including drug efflux systems, antibiotic-degrading enzymes, and alterations in drug target sites, which complicate treatment efforts (Ranganathan et al., 2024; Sakalauskienė et al., 2025). This alarming trend, coupled with a severely limited pipeline of new antibacterial compounds, underscores the urgent and unmet need to discover novel compounds with unique mechanisms of action to combat these resilient pathogens.

Extreme and underexplored environments, such as deserts, permafrost, deep-sea sediments, and peat soils, have become focal points for the bioprospecting of new antibiotics. This exploration extends to diverse biological sources, including plants, animals, and microbes, which produce a vast array of defensive and competitive compounds. These ecological niches often harbour unique microbial communities adapted to survive harsh conditions,

Cite this Article as: Mahdiyah D, Mukti BH, Darsono PV and Redjeki DSS, 2026. A novel Anti-MDR activity and in silico pharmacological profiling of 2,4-Di-tert-butylphenol from indonesian peat soil *Lysinibacillus* sp. against DNA Gyrase. International Journal of Agriculture and Biosciences 15(3): 974-983. https://doi.org/10.47278/journal.ijab/2026.014

A Publication of Unique Scientific Publishers

driving them to produce a diverse array of specialized secondary metabolites as a competitive strategy (Mahdiyah et al., 2019, Mukti, 2024; Ranganathan et al., 2024). Indonesian peat soil, characterized by high acidity, low nutrient content, high water and organic matter content, and anaerobic conditions, represents an extreme ecosystem (Sayed et al., 2020; Khoerani et al., 2023; Manalu et al., 2024; Mohamad et al., 2024) The immense microbial diversity within peatlands, including *Proteobacteria*, *Acidobacteria*, and *Actinobacteria*, remains largely untapped, thus constituting a promising reservoir for potent bioactive compounds (Liu et al., 2020; Pratiwi et al., 2021; Bandla et al., 2023; Mahdiyah et al., 2025b). Among bacterial genera thriving in diverse environments, *Lysinibacillus*—a genus noted for its metal resistance and adaptive capabilities—has recently garnered attention for its biotechnological potential (Páez-Vélez et al., 2019; Margaryan et al., 2021; Sun et al., 2024). Members of this genus have been reported to produce various antimicrobial agents, including bacteriocins and lipopeptides, effective against a range of pathogens (Jamal & Ahmad, 2022). However, the specific antimicrobial potential of a *Lysinibacillus* strain isolated from the unique environment of Indonesian peat soil, identified in this study based on 16S rRNA gene sequencing (Sanger method), particularly against clinically relevant multidrug-resistant (MDR) strains, remains underexplored and represents a significant gap in current research (Mahdiyah et al., 2025a).

A critical bottleneck in modern drug discovery is the high failure rate of lead compounds during late-stage development due to unfavourable pharmacokinetic or toxicity profiles (Prusty, 2024; Mody et al., 2025). To address this, in silico pharmacological profiling has emerged as a vital tool for the early-stage evaluation of bioactive molecules. Techniques such as prediction of Absorption, Distribution, Metabolism, Excretion, and Toxicity (ADMET) properties and molecular docking enable researchers to prioritize the most promising candidates, predict their mechanisms of action by simulating interactions with bacterial target proteins, and reduce the risk of failure in in vitro and in vivo assays. These computational approaches provide a rational framework to streamline the transition from discovery to development (Jia & Gao, 2022; Effinger et al., 2024; Suvidhi et al., 2024; Wang et al., 2024).

This study is designed to bridge this research gap by systematically investigating the antimicrobial potential of a *Lysinibacillus* strain originating from Indonesian peat soil. We hypothesize that this isolate produces broad-spectrum antibacterial compounds, including activity against clinical MDR isolates, and that its primary active metabolite will exhibit a favourable in silico pharmacological profile. Accordingly, the objectives of this study are to: (1) evaluate the broad-spectrum and anti-MDR activity of its crude extract; (2) identify the structure of the active compound via GC-MS; and (3) conduct a comprehensive *in silico* pharmacological assessment, including ADMET prediction and molecular docking, to evaluate its drug-likeness and potential mechanism of action.

MATERIALS & METHODS

Antibacterial Activity Assay using the Kirby-Bauer Disc Diffusion Method

The antibacterial activity of the crude extract from *Lysinibacillus* sp. was tested against clinical MDR isolates Methicillin-resistant *Staphylococcus aureus* (MRSA) ATCC 43300 and Extended-Spectrum Beta-Lactamases (ESBL)-producing *Escherichia coli* ATCC 35218, as well as the pathogens *Pseudomonas aeroginosa* ATCC 10145, *Cutibacterium acnes* ATCC 11827, *Staphylococcus epidermidis* ATCC 35984, and *Salmonella enterica* serovar Typhi (*S.* Typhi) ATCC 14028. Modified from Mahdiyah et al. (2020), each activated test bacterium was cultured in Mueller-Hinton Broth (MHB; HiMedia, India) and incubated at 37°C, pH 6, for 24 hours. For *C. acnes*, incubation was performed anaerobically using an anaerobic incubator at 37°C, pH 6, for48 hours. The bacterial cell suspension density was standardized to 0.5McFarland (equivalent to ~1.5 x 10^8CFU/mL). The 0.5McFarland standard was prepared by adding 1% v/v sulfuric acid (H_2SO_4; 1mL) to 1% w/v barium chloride ($BaCl_2$; 99mL), which produces a defined optical density. *Lysinibacillus* was subcultured in Tryptic Soy Broth (TSB; Sigma-Aldrich, Germany) at 37°C, pH 6, for 48hours and then centrifuged at 4000rpm for 10minutes. The cell-free supernatant was used for the antibacterial activity test. The bacterial test suspension was swabbed evenly over the entire surface of Mueller-Hinton Agar (MHA; HiMedia, India) using a sterile cotton swab, which were poured to a uniform depth of 4mm. For *C. acnes*, the medium used was Mueller-Hinton Agar enriched with 5% defibrinated blood (Infusion Agar; HiMedia, India) under anaerobic conditions. Discs impregnated with the cell-free supernatant and a 30µg chloramphenicol disc (Oxoid, UK) were used as positive controls. The discs were then placed on the inoculated agar and incubated at 37°C (24hours for aerobic bacteria; 48hours anaerobic for *C. acnes*). The diameter of the inhibition zone was measured after incubation. The antibacterial activity was interpreted according to CLSI breakpoints (CLSI, 2012) for the positive control chloramphenicol to ensure assay validity. This screening using a single biological sample, the results are presented as the raw inhibition zone diameter from a single experiment (n=1) without statistical analysis.

Gas Chromatography-Mass Spectrometry (GC-MS) and Target Compound Selection

Volatile and semi-volatile compounds in the cell-free supernatant obtained from the *Lysinibacillus* sp. culture were analyzed using GC-MS via the E-Layanan Sains (ELSA) of the Badan Riset dan Inovasi Nasional (BRIN), Jakarta, Indonesia. GC-MS analysis was conducted using an Agilent 7890B GC system coupled with a 5977A Mass Selective Detector (MSD) equipped with an HP-5MS capillary column (30m × 0.25mm i.d., 0.25µm film thickness; Agilent Technologies). Helium was used as the carrier gas at a constant flow rate of 1.0mL/min, with the injector temperature set at 250°C in split mode (10:1) and an injection volume of 1µL. The oven temperature program started at 60°C (2min hold), increased to 280°C at 10°C/min, and was held for 10min. The MS was operated in

electron impact (EI) mode at 70eV, with an ion source temperature of 230°C, quadrupole temperature of 150°C, and a scan range of 40–500m/z. Spectral identification was performed using the NIST23 mass spectral library**.** Compounds identified from the GC-MS results were evaluated based on the percentage of peak area and the similarity index with reference spectra. Only compounds with a similarity index >90% and a peak area >1% were considered for further analysis. Compounds with documented antibacterial activity in the literature were subsequently selected for *in silico* testing.

In Silico Pharmacodynamic Evaluation

The pharmacodynamic evaluation, including drug-likeness and physicochemical properties of the selected compound, was performed using the SwissADME (2017) (http://www.swissadme.ch). The analyzed parameters of Lipinski's Rule of Five included a molecular weight <500Dalton, partition coefficient (Log P) <5, number of hydrogen bond donors (HBD) <5, number of hydrogen bond acceptors (HBA) <10, and Topological Polar Surface Area (TPSA) < 140Å^2. If the target compound met ≥4 of the 5 Lipinski criteria, it proceeded to further testing.

In Silico Toxicity Analysis

Compound toxicology was predicted using the ProTox 3.0 (http://tox.charite.de, accessed on 9 August 2025) (Banerjee et al., 2024). The analyzed parameters included the LD_{50} value, hepatotoxicity, carcinogenicity, immunotoxicity, mutagenicity, and cytotoxicity, which were categorized as active or inactive.

In Silico Pharmacokinetic Analysis

The pharmacokinetic profile was predicted using the pkCSM web server (http://biosig.unimelb.edu.au/pkcsm, accessed on 9 August 2025) (Pires et al., 2015). The evaluated parameters included:

– **Absorption**

Absorption is the process by which an active compound enters the systemic circulation from its site of administration. The prediction of a compound's absorption level utilized several parameters:

a. Human Intestinal Absorption (HIA) was used to estimate the compound's ability to pass through the human intestinal tract. The obtained value reflects a combination of bioavailability and absorption rate, calculated based on the excretion ratio via urine, bile, and feces. Molecules with absorption ≤ 30% were considered poorly absorbed.

b. Caco-2 cell permeability was predicted using a model built from 674 drug molecules with known Caco-2 permeability values, predicting the logarithm of the apparent permeability coefficient (log Papp; in log cm/s). Caco-2 cells are human colorectal adenocarcinoma epithelial cells widely used as an in vitro model of the human intestinal mucosa to predict the absorption of orally administered drugs. A log Papp value > 0.90 indicates high permeability.

c. Water Solubility (Log S) reflects the solubility of the molecule in water at 25 °C. Lipophilic drugs are generally less well absorbed compared to water-soluble drugs, particularly when administered enterally. This model was built using experimental data from 1708 water solubility measurements. A Log S value < -4 indicates low solubility, -4 to -2 indicates moderate solubility, and > -2 indicates good solubility.

– **Distribution**

Distribution is the process of drug transfer from the systemic circulation to tissues and body fluids. In the *in silico* prediction using the pkCSM web server, the distribution process of the compound was evaluated through three main parameters: the volume of distribution in humans (*Volume of Distribution at steady state* or VDss Human), blood-brain barrier permeability (BBB permeability) and central nervous system permeability (CNS permeability).

a. Volume of Distribution (VDss) was predicted using a Gradient Boosting model based on a dataset of 1120 compounds. A log VDss value < -0.15 indicates limited distribution, while > 0.45 indicates wide distribution.

b. Blood-Brain Barrier Permeability (Log BB) is an important parameter to consider for helping to reduce side effects and toxicity or to enhance the efficacy of drugs whose pharmacological activity is within the brain. Log BB was predicted using a Gaussian Process model based on a dataset of 120 compounds. A Log BB value > 0.3 indicates good permeability, while < -1.0 indicates poor permeability.

c. CNS Permeability (Log PS) was used to evaluate a compound's ability to penetrate the central nervous system. Log PS was predicted using a Gaussian Process model based on a dataset of 110 compounds. A Log PS value > -2 indicates good permeability, while < -3 indicates an inability to penetrate the CNS.

– **Metabolism**

Metabolism is the process of biotransformation of a drug compound into active metabolites that can exert pharmacological effects, or into inactive metabolites ready for elimination from the body. This process primarily occurs in the liver, the main organ containing various metabolic enzymes, including those from the cytochrome P450 family. Inhibition of cytochrome P450 enzymes was predicted for isoforms CYP2D6 and CYP3A4 using a Support Vector Machine (SVM) model. The output is stated as "Yes" (inhibitor) or "No" (non-inhibitor).

– **Excretion**

Excretion is the process of drug elimination from the body, which primarily occurs through the kidneys and is excreted in urine. Besides the renal pathway, drug excretion can also occur through the lungs, skin, and exocrine secretions such as sweat and saliva. The evaluation of excretion parameters included:

a. Total Clearance reflects the combined rate of elimination through hepatic metabolism, biliary secretion, and renal excretion. The higher the total clearance value, the faster the drug concentration declines in the blood plasma. Total clearance was predicted using a Gradient Boosting model based on a dataset of 950 compounds. A high value indicates rapid elimination.

b. The organic cation transporter 2 (OCT2) inhibition, plays a crucial role in the disposition and elimination of various drugs and endogenous compounds through renal filtration. OCT2 inhibition was predicted using a Support Vector Machine model based on a dataset of 191 compounds.

Molecular Docking

Molecular docking was performed to predict the interaction between the ligand compound and DNA gyrase subunit B (receptor). The protein structure was downloaded from the Protein Data Bank (https://www.rcsb.org, accessed on 10 August 2025). Protein preparation involved the removal of water molecules and the native ligand using PyMOL 2.6, followed by the addition of hydrogen atoms and charges using AutoDock Tools 1.5.7. Validation of the docking method was performed by redocking the native ligand and was considered valid if the Root Mean Square Deviation (RMSD) value was ≤ 2.0 Å. Docking simulation was conducted using AutoDock Vina 1.1.2 with grid box parameters encompassing the receptor's active site. The binding affinity value (kcal/mol) and molecular interactions (hydrogen bonds, hydrophobic and electrostatic interactions) were analyzed using Discovery Studio Visualizer.

Ligand preparation was performed using the PyRx software (version 0.8) and its integrated Open Babel tool (version 3.1.1, accessed in 10 August 2025). The 3D structure of 2,4-di-tert-butylphenol (2,4-DTBP; PubChem CID: 7311) was retrieved from the PubChem database in SDF format. The ligand was then imported into PyRx and subjected to energy minimization using the MMFF94 force field. During this automated process, PyRx assigned Gasteiger charges and detected rotatable bonds to generate the final, optimized structure in PDBQT format. The most probable protonation state at physiological pH (7.4) was selected for docking.

RESULTS AND DISCUSSION

Broad-Spectrum and Anti-MDR Activity

The cell-free supernatant of the *Lysinibacillus* sp. isolate demonstrated broad-spectrum inhibitory activity, encompassing both Gram-negative and Gram-positive bacteria, as well as clinical Multi-Drug Resistant (MDR) isolates. Results from the Kirby-Bauer disc diffusion assay revealed the presence of clear zones (zones of inhibition) surrounding the discs impregnated with the supernatant across all tested bacterial strains (Fig. 1). Table 1 reveals variations in the resulting inhibition zone diameters. The highest inhibition zone diameters were observed against *S.* Typhi (16.23mm) and MRSA (16.16mm). Activity was also demonstrated against *P. aeroginosa* (12.1 mm) and ESBL-producing *E. coli* (11.76mm). Meanwhile, activity against *S. epidermidis* (10.68mm) and *C. acnes* (9.74mm) appeared lower than that of chloramphenicol (30µg).

These findings confirm the potential of the *Lysinibacillus* isolate from its unique source, the peat soil of South Kalimantan, as a producer of broad-spectrum antibacterial compounds. Its ability to inhibit the growth of both Gram-negative (ESBL *E. coli*, *P. aeroginosa*, *S.* Typhi) and Gram-positive (MRSA, *S. epidermidis*, *C. acnes*) bacteria suggests that the produced secondary metabolites possess a mechanism of action that may target conserved cellular structures or processes common to both bacterial groups (Kastrat & Cheng, 2024; Pendyukhova et al., 2024).

Table 1: Inhibition zones of *Lysinibacillus* supernatant against pathogens.

Patogens	Inhibition zone diameter (mm)	
	Supernatant	Chloramphenicol (30µg)
ESBL *E. coli*	11.76	12.51 (Resistant)
MRSA	16.16*	10.72 (Resistant)
S. epidermidis	10.68	13.34 (Resistant)
S. Thypi	16.23	16.64 (Intermediet)
P. aeroginosa	12.10	11.64 (Resistant)
C. acnes	9.74	12.21 (Resistant)

Note: * A noteworthy result where the supernatant's activity exceeded that of the chloramphenicol control.

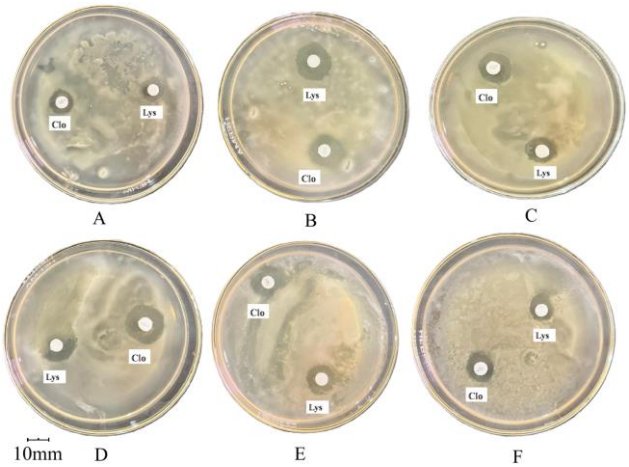

Fig. 1: Antibacteria activity of *Lysinibacillus* (denoted as Lys) with positive control Chloramphenicol (Clo) against MDR and pathogenic bacteria: A) ESBL *E. coli*; B) MRSA; C) *S. epidermidis*; D) *S.* Typhi; E) *P. aeroginosa*; F) *C. acnes*.

The most promising finding is the supernatant's potent activity against clinical MDR isolates, particularly MRSA and ESBL-producing *E. coli*. Notably, the supernatant produced a larger inhibition zone against MRSA (16.16mm) compared to the chloramphenicol control (10.72mm), suggesting that the bioactive compounds produced by this *Lysinibacillus* sp. may circumvent the specific resistance mechanisms of this pathogen (Lade et al., 2022; Abebe & Birhanu, 2023). The activity against ESBL-producing *E. coli*, although slightly lower than chloramphenicol, remained significant and suggests that the compound(s) are not readily degraded by beta-lactamase enzymes, the primary resistance mechanism in these bacteria (Al-Hasso & Mohialdeen, 2023; Chaudhary et al., 2023; Li et al., 2023). The variation in inhibition zone diameters among the different bacteria can be attributed to several factors. First, the difference in cell wall structure between Gram-positive and Gram-negative bacteria. The lipopolysaccharide outer membrane of the Gram-negative cell wall often presents a more formidable barrier for antibacterial molecules to penetrate. Second, differences in membrane permeability and the presence of species-specific efflux systems (efflux pumps) can influence the intracellular accumulation of the antibacterial compound(s). Third, the activity spectrum of the antibacterial compound(s) itself may be more specific to certain metabolic pathways, the presence or susceptibility of which varies between bacterial species (Vaara, 2020; Vergalli et al., 2020; Leus et al., 2023; Maher & Hassan, 2023; Shahanawaz et al., 2024).

Table 2: Candidate secondary metabolite compounds for *in silico* testing

Retention time (min.)	Compound name	Formula	Area	Similarity index (%)	Antibacterial activity
13.3629	Methyl cinnamate ((E)-)	$C_{10}H_{10}O_2$	1228650	92.4	Yes [1]
14.7978	2,4-Di-tert-butylphenol	$C_{14}H_{22}O$	1882246	97.4	Yes [2]
17.9782	Benzyl Benzoate	$C_{14}H_{12}O_2$	1386664	92.7	Yes [3]

[1] (Wulandari et al., 2022); [2] (Rouvier et al., 2024); [3] (Korany & Aboelhadid, 2024)

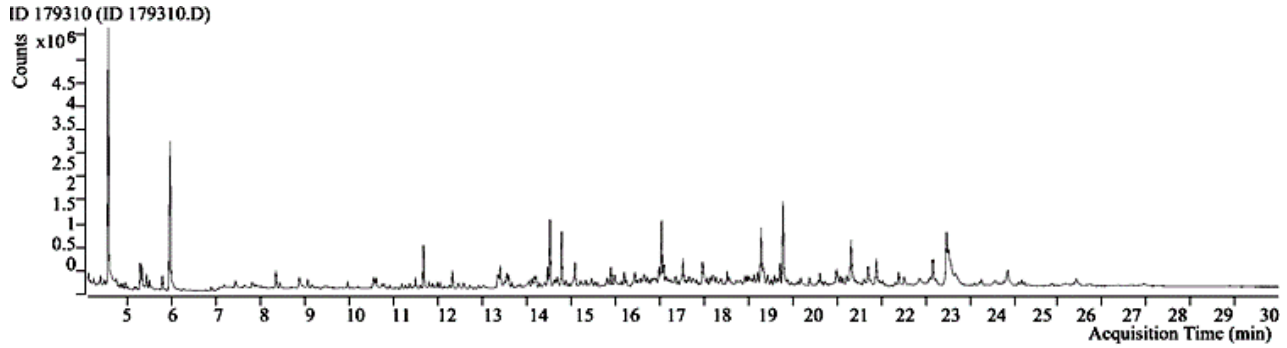

Fig. 2: TIC of the *Lysinibacillus* sp. cell-free supernatant.

Identification of Antibiotic Compound

The cell-free supernatant obtained from the *Lysinibacillus* sp. culture was analyzed for its volatile and semi-volatile compound content using GC-MS. The resulting Total Ion Chromatogram (TIC) revealed a complex metabolic profile with several dominant peaks eluting between 5 and 30minutes, as presented in Fig. 2.

TIC from the *Lysinibacillus* sp. cell-free supernatant led to the exclusion of compounds such as alkyl esters (e.g., Acetic acid, butyl ester) and alkyl ethers (e.g., Ethanol, 2-butoxy-), which are common industrial solvents, as well as long-chain alkanes (e.g., Heneicosane), which are components of mineral oils, from the pool of potential authentic secondary metabolites. Three compounds with a high probability of being true bacterial metabolites, further supported by documented strong antibacterial activity in the literature, were selected as candidates for in silico testing (Table 2).

Among the three candidates, 2,4-Di-*tert*-butylphenol (2,4-DTBP) emerged as the most promising compound and was selected as the primary focus for this study, based on the following scientific rationales:

a. Strong and specific track record as a bacterial metabolite

Unlike other compounds which may originate from alternative sources, 2,4-DTBP is widely recognized and consistently reported as a secondary metabolite from various bacterial genera, including *Bacillus, Pseudomonas, Streptomyces*, and *Lysinibacillus*. Its production is frequently associated with antagonistic and competitive mechanisms in the environment (Ortiz & Sansinenea, 2023; Velusamy et al., 2024; Mahdiyah et al., 2025a). This minimizes its likelihood of being a contaminant and strengthens its status as an authentic compound produced by the investigated *Lysinibacillus* sp. isolate.

b. Multifaceted and potent antibacterial mechanism of action

2,4-DTBP is not merely bacteriostatic but also exhibits a multifaceted mechanism of action, which is highly desirable for countering antibiotic resistance:

– 2,4-DBP inhibits quorum sensing, reducing virulence factor secretion and biofilm formation, which are critical for bacterial pathogenicity (Mishra et al., 2020)

– Affects membrane permeability and induces reactive oxygen species production, contributing to bacterial cell death (Yang et al., 2024)

– The compound significantly reduces biofilm formation, enhancing the efficacy of existing antibiotics (Mishra et al., 2020)

– Demonstrated effective inhibition of growth, especially against antibiotic-resistant strains (Rouvier et al., 2024; Mahdiyah et al., 2025b)

c. Feasibility as an in silico target

The relatively small molecular structure of 2,4-DTBP, featuring a reactive phenolic functional group, makes it an ideal candidate for molecular docking studies. This compound can be docked onto various target proteins involved in essential enzymes of pathogenic bacteria. Predicting its interactions with target proteins can provide valuable mechanistic insights that support the biological data.

d. Identification abundance and purity

The compound 2,4-di-tert-butylphenol (CAS 96-76-4) was detected at retention time (RT) = 14.7978min with a match score of 97.4%. The main EI ions were m/z 57, 115, 163, 191, and 206, consistent with literature spectra for 2,4-DTBP. The retention index (RI) could not be determined due to the absence of alkane standards, and no authentic standard of 2,4-DTBP was analyzed. The corresponding EI mass spectrum is provided in the Supplementary Material.

Based on the aforementioned considerations, 2,4-DTBP was established as the primary bioactive compound candidate hypothesized to be responsible for the antibacterial activity of the *Lysinibacillus* sp. supernatant. This compound was prioritized for molecular docking simulations to predict its binding affinity and inhibitory mechanism against target proteins in pathogenic bacteria.

Pharmacodynamics: Drug-Likeness and Physicochemical Properties

The predicted drug-likeness and physicochemical properties of 2,4-DTBP, obtained using the SwissADME platform, are presented in Table 3. The analysis revealed that 2,4-DTBP possesses a molecular weight (MW) of 206.32Dalton, a partition coefficient (Log P) value of 3.99,

one hydrogen bond donor (HBD), one hydrogen bond acceptor (HBA), and a Topological Polar Surface Area (TPSA) value of 20.23Å^2. According to the parameters of Lipinski's Rule of Five, 2,4-DTBP satisfied all criteria: MW <500Dalton, Log P <5, HBD ≤5, and HBA ≤10. Thus, the compound demonstrated full compliance with Lipinski's rules (score 5/5), indicating favorable drug-like characteristics and a high potential for oral bioavailability.

Table 3: Pharmacodynamic prediction for the 2,4-DTBP compound.

Parameter	Value	Lipinski's Criteria	Status
MW	206.32Dalton	<500Dalton	Satisfied
Log P	3.99	<5	Satisfied
HBA	1	≤10	Satisfied
HBD	1	≤5	Satisfied
TPSA	20.23Å^2	<140Å^2	Satisfied
Lipinski's Rule	Yes	5/5	

Compliance of 2,4-DTBP with all of Lipinski's rules represents a highly significant initial indicator for the development of a novel antibacterial compound. The low molecular weight (206.32Dalton) and small TPSA value (20.23Å^2) demonstrate the compound's excellent potential for diffusing through biological membranes, penetrating the blood-brain barrier, and eliciting an effect—an essential prerequisite for reaching its target site of action within bacterial cells. The Log P value, approaching 4 (3.99), indicates balanced lipophilicity, which not only facilitates penetration through the lipid bilayer of membranes but also ensures sufficient water solubility for transport within biological systems. Fulfillment of all these criteria not only predicts good oral bioavailability but also strengthens the viability of 2,4-DTBP as a feasible drug candidate worthy of proceeding to molecular docking simulations to validate its interactions with target proteins and to study its mechanism of action in greater depth.

Toxicity Properties

The predicted toxicity results for the compound 2,4-Di-*tert*-butylphenol (2,4-DTBP), obtained using the ProTox 3.0 server, are presented in Table 4. Based on an LD_{50} value of 700mg/kg, the compound 2,4-DTBP is classified under Category 4 according to the Globally Harmonized System (GHS) (Banerjee et al., 2024). This prediction was made with an accuracy and similarity level of 100%. Furthermore, the prediction results for various organ-specific toxicity parameters (Table 4) indicated that 2,4-DTBP was predicted to be inactive for all tested toxicity endpoints, namely hepatotoxicity, carcinogenicity, immunotoxicity, mutagenicity, and cytotoxicity.

Table 4: Predicted LD_{50} value for the compound 2,4-Di-*tert*-butylphenol.

LD_{50}	Classification	Accuracy (%)	Similarity (%)
700 mg/kg	Category 4	100	100

The in-silico toxicity prediction results provide a preliminarily favourable overview of the safety profile of the 2,4-DTBP compound. An LD_{50} value of 700mg/kg, which places it in Category 4, indicates that the compound exhibits low to moderate acute toxicity. More significantly, the prediction results consistently showed inactive for all forms of organ-specific toxicity and cellular toxicity, including hepatotoxicity and carcinogenicity. This suggests that, at a molecular level, the compound is predicted to lack strong binding affinity for receptors or enzymes responsible for these toxic effects. The combination of excellent drug-likeness properties (conforming to Lipinski's rules) and this low toxicity profile further strengthens the potential of 2,4-DTBP as a viable antibacterial candidate worthy of further development. These predictions, supported by 100% accuracy and similarity, provide greater confidence in the reliability of the results, although further validation through in vitro and in vivo testing remains absolutely necessary to confirm its overall safety.

Pharmacokinetic Properties

The predicted pharmacokinetic profile of the 2,4-DTBP compound, obtained using the pkCSM server, is presented in Table 5. The compound exhibited high human intestinal absorption (HIA = 92.03%), indicating good oral bioavailability, and strong Caco-2 permeability (log Papp = 1.67 × 10^{-6}cm/s), suggesting efficient intestinal membrane transport. Its water solubility (log S = −3.92mol/L) reflects moderate solubility under physiological conditions. In terms of distribution, 2,4-DTBP showed a wide apparent volume of distribution (VDss = 0.61L/kg), suggesting moderate tissue penetration, and a blood–brain barrier permeability (log BB = 0.48) value indicative of potential central nervous system (CNS) access, although its CNS permeability (log PS = −0.85) remains low, implying limited CNS accumulation. Metabolic predictions indicated that 2,4-DTBP is not an inhibitor of cytochrome P450 isoenzymes CYP2D6 and CYP3A4, which reduces the risk of metabolic drug–drug interactions. For excretion, the compound displayed a moderate total clearance (0.76mL/min/kg), suggests an elimination half-life that is neither too rapid nor too prolonged, which could support a less frequent dosing regimen, and was predicted not to inhibit the renal OCT2 transporter. Overall, the in silico pharmacokinetic properties of 2,4-DTBP, characterized by excellent absorption and distribution along with low potential for drug interactions and toxicity, further strengthen its viability as a promising antibacterial candidate worthy of further development.

Docking Molecular

a. Protein preparation

The target protein used for molecular docking analysis was obtained from the Protein Data Bank (PDB). Preparation of the target protein involved separation of the native ligand from other molecules, including water molecules.

b. Docking validation

The molecular docking protocol was validated to ensure its reliability in predicting ligand binding modes. This was achieved by re-docking the native co-crystallized ligand into the binding site of the DNA gyrase subunit B receptor (PDB ID: 1KZN). The validation yielded excellent results, with a Root Mean Square Deviation (RMSD) value of 0Å between the redocked and the original crystallographic poses, confirming the accuracy of the methodology.

The docking simulations were performed using AutoDock Vina within the PyRx software (version 0.8) environment, utilizing the Vina Wizard for setup. The grid box was strategically centered on the active site to

Table 5: In Silico Pharmacokinetic Profile of 2,4-DTBP

Category	Specific Parameter	Predicted Value	Interpretation
Absorption	Human Intestinal Absorption (HIA)	92.03%	High oral absorption
	Caco-2 Permeability (log Papp)	1.67 x 10^{-6}cm/s	Strong membrane permeability
	Water Solubility (log S)	-3.92mol/L	Moderate solubility
Distribution	Volume of Distribution (VDss, log L/kg)	0.61L/kg	Moderate tissue distribution
	Blood-Brain Barrier Permeability (log BB)	0.48	Moderate BBB permeability
	CNS Permeability (log PS)	-0.85	Low CNS penetration
Metabolism	CYP2D6 Inhibitor	No	Non-inhibitor
	CYP3A4 Inhibitor	No	Non-inhibitor
Excretion	Total Clearance	0.76mL/min/kg	Moderate clearance rate

Table 6: Docking validation parameter

Macromolecule	Gridbox						RMSD (Å)
	Center			Dimensi			
	X	Y	Z	X	Y	Z	
Receptor	12.325	-3.221	-12.108	44.843	63.132	52.976	0

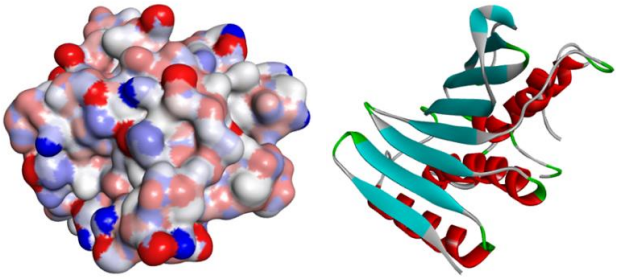

Fig. 3: DNA gyrase (left) and subunit B (right) #D structure.

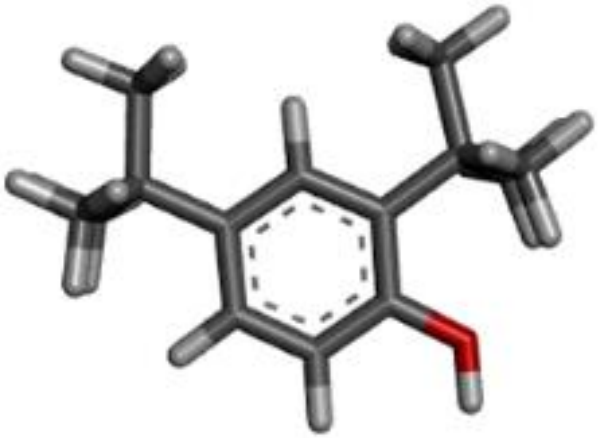

Fig. 4: 2,4-DTBP 3D structure.

encompass key residues known to be critical for ligand binding, such as LYS11, VAL12, LYS14, GLY15, LEU16, VAL43, ASN46, ALA47, VAL71, ASP73, ILE78, THR96, VAL97, LEU98, HIS99, VAL 120, SER121, THR165, VAL167. The box dimensions (44.843 Å x 63.132 Å x 52.976 Å; Table 6) were chosen to be sufficiently large to allow for full rotational and translational freedom of the ligand during the docking process. An exhaustiveness value of 8 was employed, as this default setting provided a robust balance between computational efficiency and search thoroughness for this system.

c. Binding affinity value

Based on the molecular docking simulation results, the compound 2,4-di-tert-butylphenol demonstrated the ability to interact with the target receptor, as indicated by a binding affinity value of -5.9kcal/mol. A more negative value signifies a stronger binding interaction. Generally, a binding affinity value ≤ -5.0kcal/mol is considered to indicate good binding affinity (Asiat et al., 2020; Forli et al., 2016; Trott & Olson, 2010). Therefore, the obtained value of -5.9kcal/mol suggests that this compound has a strong potential to bind to the target receptor and is likely to inhibit its biological function, albeit not as potent as clinical DNA gyrase inhibitors such as fluoroquinolones (which typically exhibit values < -8kcal/mol) (Luan & Drlica, 2018).

d. Molecular docking visualization

The target protein, DNA gyrase (Fig. 3), and the ligand structure of 2,4-DTBP (Fig. 4) were first visualized to establish the docking framework. The three-dimensional visualization in Fig. 5 illustrates the position of 2,4-DTBP within the binding pocket of the DNA gyrase enzyme, while the two-dimensional visualization in Fig. 6 confirms dominant hydrophobic interactions with key residues. The predominance of hydrophobic interactions is consistent with the lipophilic nature of 2,4-DTBP (Belghit et al., 2016), facilitating its penetration into the hydrophobic pocket of the target protein.

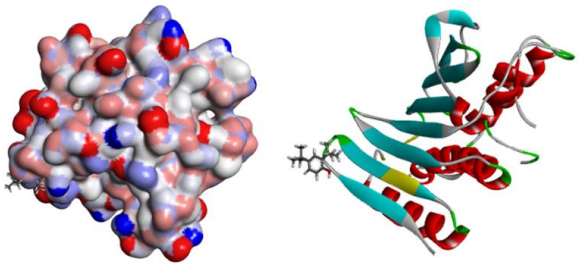

Fig. 5: Three-dimensional (left) and two-dimensional (right) visualization of molecular docking results between 2,4-DTBP and DNA gyrase subunit B, illustrating ligand positioning and key molecular interactions.

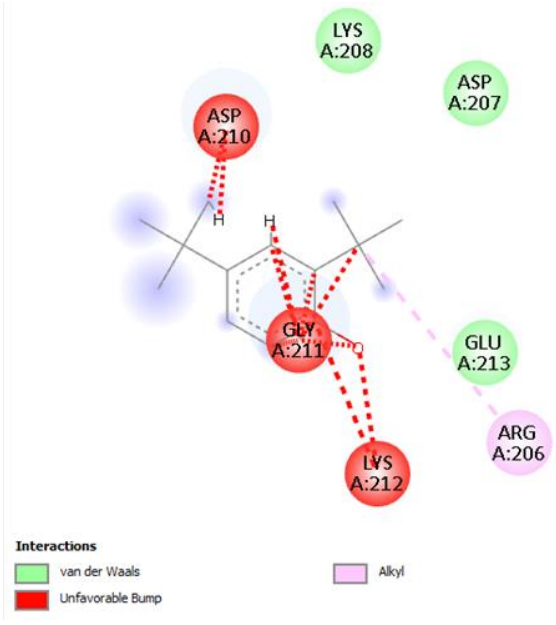

Fig. 6: Two-dimensional visualization of molecular interactions between 2,4-DTBP and key residues in the DNA gyrase subunit B binding pocket.

The 2D visualization reveals that the interactions between 2,4-DTBP and DNA gyrase subunit B are dominated by van der Waals forces with key residues LYS A:208, ASP A:210, GLY A:211, GLU A:213, ARG A:206, and LYS A:212. Although several unfavorable bumps are observed, which may slightly reduce binding stability, the presence of hydrophobic (alkyl) interactions with surrounding hydrophobic residues indicates that the binding mechanism is primarily driven by lipophilic compatibility. This interaction pattern aligns with the lipophilic nature of 2,4-DTBP (Log P = 3.99) and supports the hypothesis that the compound potentially inhibits DNA gyrase function by competing with natural substrates in the enzyme's hydrophobic pocket. However, the absence of strong hydrogen or electrostatic bonds explains why the binding affinity (-5.9kcal/mol) is lower than that of clinical inhibitors such as fluoroquinolones, which form covalent bonds with catalytic residues.

DNA gyrase subunit B is an essential antibacterial target responsible for bacterial DNA supercoiling. Inhibition of this enzyme disrupts DNA replication processes, leading to inhibited bacterial growth or cell death (Collin et al., 2011; Higgins, 2013; Dötsch, 2024). The visualization data support the hypothesis that 2,4-DTBP may act as a DNA gyrase inhibitor. These results strengthen the connection between the antagonistic data of the *Lysinibacillus* isolate (Fig. 1) and the GC-MS identification (Fig. 2) with a potential mechanism of action that explains the broad-spectrum activity and ability to inhibit MDR pathogens, including MRSA and ESBL-producing *E. coli*. Thus, the combination of experimental data and computational simulations confirms the role of 2,4-DTBP as the primary bioactive metabolite responsible for the antibacterial activity of this isolate.

Future research should focus on several aspects. First, the isolation and purification of 2,4-DTBP from *Lysinibacillus* sp. cultures using preparative chromatography followed by structural validation using advanced spectroscopic methods (NMR, FTIR, LC-MS/MS) is essential to confirm the compound's identity and purity. Second, further in vitro testing against various MDR strains, including the ESKAPE pathogen panel, is necessary to strengthen the evidence of its broad-spectrum activity and clinical potential. Third, in vivo toxicity and efficacy studies in infection model animals should be conducted to validate the safety and pharmacodynamic profiles predicted in silico. Fourth, a more detailed exploration of the molecular mechanism of action through target validation assays and omics approaches could help elucidate the biological pathways affected by 2,4-DTBP. Finally, comparative studies with other natural antibacterial compounds from Indonesian peat soil are also recommended to expand bioprospecting potential and support the development of novel antibiotic candidates from this unique ecosystem.

Conclusion

This study confirms that *Lysinibacillus* sp., isolated from South Kalimantan peat soil, represents a potential source of secondary metabolites with broad-spectrum antibacterial activity and the ability to inhibit multi-drug resistant (MDR) pathogens. The culture supernatant demonstrated efficacy against MRSA and ESBL-producing *Escherichia coli*, with competitive inhibition zones that even exceeded those of the control antibiotic for MRSA. GC-MS analysis identified 2,4-DTBP with a high similarity index (97.4%), reinforcing its status as an authentic metabolite of this isolate. The pharmacodynamic profile indicated that 2,4-DTBP fully complies with Lipinski's rules, suggesting favorable drug-like properties and potential oral bioavailability. *In silico* toxicity predictions classified the compound as safe, with an LD_{50} of 700mg/kg (Category 4) and negative results for all organ-specific toxicity parameters. Pharmacokinetic evaluation revealed high intestinal absorption, extensive tissue distribution, and no inhibition of key CYP enzymes or renal transporters, supporting its pharmaceutical development potential. Molecular docking results demonstrated a binding affinity of -5.9kcal/mol against DNA gyrase subunit B, with dominant hydrophobic interactions consistent with the lipophilic nature of 2,4-DTBP. Three- and two-dimensional visualizations confirmed stable interactions within the enzyme's binding pocket, supporting the hypothesis that the antibacterial mechanism of action of 2,4-DTBP involves inhibition of bacterial DNA replication.

DECLARATIONS

Funding: This research was funded by the Directorate of Research and Community Service, Ministry of Higher Education, Science, and Technology of the Republic of Indonesia under the Master Contract No. 132/C3/DT.05.00/PL/2025 (2025).

Acknowledgement: The authors acknowledge to Directorate of Research and Community Service, Ministry of Higher Education, Science, and Technology of the Republic of Indonesia, through the Penelitian Fundamental Reguler, and Universitas Sari Mulia for the institutional support, facilities, and resources that were essential for the successful execution of this research.

Conflict of Interest: All authors declare no conflict of interest.

Data Availability: The authors declare that the data supporting the findings of this study are available within the paper and its Supplementary Information files. Should any raw data files be needed in another format are available from the corresponding author upon reasonable request.

Ethics Statement: The authors declare that no ethical approval was required for this *in silico* study.

Author's Contribution: Dede Mahdiyah: Conceptualization, Methodology, Data Analysis, Interpretation. Bayu Hari Mukti: Conceptualization, Methodology, Data collection, Data Analysis, Writing and

revision of manuscript. Putri Vidiasari Darsono: Methodology, Data Collection, Data Analysis. Dwi Sogi Sri Redjeki: Analysis, interpretation, writing, and revision manuscript.

Generative AI Statement: The authors declare that no Gen AI/DeepSeek was used in the writing/creation of this manuscript.

Publisher's Note: All claims stated in this article are exclusively those of the authors and do not necessarily represent those of their affiliated organizations or those of the publisher, the editors, and the reviewers. Any product that may be evaluated/assessed in this article or claimed by its manufacturer is not guaranteed or endorsed by the publisher/editors.

REFERENCES

Abebe, A., & Birhanu, A. (2023). Methicillin-resistant *Staphylococcus aureus*: Molecular mechanisms underlying drug resistance development and novel strategies to combat. *Infection and Drug Resistance, 16*, 7641–7662.

Al-Hasso, M., & Mohialdeen, Z. (2023). A review of extended-spectrum β-lactamases: Definition and types. *Kirkuk University Journal–Scientific Studies, 18*(1), 44–61. https://doi.org/10.32894/kujss.2023.137295.1090

Asiat, N., Ayipo, Y.O., Komolafe, D.I., Solihu, S., Bamidele, B., Alabi, M.A., Balogun, A.-A., Abdulazeez, A.T., & Mordi, M.N. (2021). Phytochemical screening and *in silico* pharmacological profiling of ethanolic extract of *Aframomum melegueta* for prostate carcinoma. *Journal of Applied Pharmaceutical Science, 11*(7), 132–145. https://doi.org/10.7324/JAPS.2021.110715

Bandla, A., Mukhopadhyay, S., Mishra, S., Sudarshan, A.S., & Swarup, S. (2023). Genome-resolved carbon processing potential of tropical peat microbiomes from an oil palm plantation. *Scientific Data, 10*(1), 373. https://doi.org/10.1038/s41597-023-02267-z

Banerjee, P., KemmLer, E., Dunkel, M., & Preissner, R. (2024). ProTox 3.0: A webserver for the prediction of toxicity of chemicals. *Nucleic Acids Research, 52*(W1), W513–W520. https://doi.org/10.1093/nar/gkae303

Belghit, S., Driche, E. H., Bijani, C., Zitouni, A., Sabaou, N., Badji, B., & Mathieu, F. (2016). Activity of 2,4-Di-tert-butylphenol produced by a strain of Streptomyces mutabilis isolated from a Saharan soil against Candida albicans and other pathogenic fungi. *Journal de Mycologie Médicale, 26*(2), 160–169. https://doi.org/10.1016/j.mycmed.2016.03.001

Chaudhary, M.K., Jadhav, I., & Banjara, M.R. (2023). Molecular detection of plasmid-mediated *blaTEM*, *blaCTX-M*, and *blaSHV* genes in extended-spectrum β-lactamase (ESBL) *Escherichia coli* from clinical samples. *Annals of Clinical Microbiology and Antimicrobials, 22*(1), 33. https://doi.org/10.1186/s12941-023-00584-0

Clinical and Laboratory Standards Institute (CLSI) (2012). *Performance standards for antimicrobial disk susceptibility tests* (11th ed.; CLSI document M02-A11). Clinical and Laboratory Standards Institute.

Collin, F., Karkare, S., & Maxwell, A. (2011). Exploiting bacterial DNA gyrase as a drug target: Current state and perspectives. *Applied Microbiology and Biotechnology, 92*(3), 479–497. https://doi.org/10.1007/s00253-011-3557-z

Dötsch, V. (2024). Rapid, DNA-induced interface swapping by DNA gyrase. *eLife, 12*, RP86722. https://doi.org/10.7554/eLife.86722.3.sa0

Effinger, A., O'Driscoll, C.M., McAllister, M., & Fotaki, N. (2024). *In vitro* and *in silico* ADME prediction. In A. Talevi & P. A. Quiroga (Eds.), *ADME processes in pharmaceutical sciences* (pp. 337–366). Springer Nature Switzerland. https://doi.org/10.1007/978-3-031-50419-8_15

Forli, S., Huey, R., Pique, M.E., Sanner, M.F., Goodsell, D.S., & Olson, A.J. (2016). Computational protein–ligand docking and virtual drug screening with the AutoDock suite. *Nature Protocols, 11*(5), 905–919. https://doi.org/10.1038/nprot.2016.051

Higgins, N.P. (2013). Gyrase. In *Brenner's encyclopedia of genetics* (pp. 374–377). Elsevier. https://doi.org/10.1016/B978-0-12-374984-0.00670-7

Jamal, Q.M.S., & Ahmad, V. (2022). Lysinibacilli: A biological factories intended for bio-insecticidal, bio-control, and bioremediation activities. *Journal of Fungi, 8*(12), 1288. https://doi.org/10.3390/jof8121288

Jia, L., & Gao, H. (2022). Machine learning for *in silico* ADMET prediction. *Methods in Molecular Biology, 2390*, 447–460. https://doi.org/10.1007/978-1-0716-1787-8_20

Kastrat, E., & Cheng, H.-P. (2024). *Escherichia coli* has an undiscovered ability to inhibit the growth of both Gram-negative and Gram-positive bacteria. *Scientific Reports, 14*(1), 7420. https://doi.org/10.1038/s41598-024-57996-x

Khoerani, A., Iskandar, Sofyan, A., Sumarna, T., Amalia, D., & Sulaiman, S. (2023). Laboratory testing-based characterization of peat in Palangkaraya, Central Kalimantan. *Technium: Romanian Journal of Applied Sciences and Technology, 16*, 26–33. https://doi.org/10.47577/technium.v16i.9952

Korany, A.M., & Aboelhadid, S.M. (2024). Efficacy of caprylic acid, lauric arginate, benzyl alcohol, benzyl benzoate, and methyl benzoate against *Staphylococcus aureus* biofilms on stainless steel surfaces. *Food Control, 161*, 110385. https://doi.org/10.1016/j.foodcont.2024.110385

Lade, H., Joo, H.-S., & Kim, J.-S. (2022). Molecular basis of non-β-lactam antibiotic resistance in *Staphylococcus aureus*. *Antibiotics, 11*(10), 1378. https://doi.org/10.3390/antibiotics11101378

Leus, I.V., Adamiak, J., Chandar, B., Bonifay, V., Zhao, S., Walker, S.S., Squadroni, B., Balibar, C.J., Kinarivala, N., Standke, L.C., Voss, H.U., Tan, D.S., Rybenkov, V.V., & Zgurskaya, H.I. (2023). Functional diversity of Gram-negative permeability barriers reflected in antibacterial activities and intracellular accumulation of antibiotics. *Antimicrobial Agents and Chemotherapy, 67*(2), e01377-22. https://doi.org/10.1128/aac.01377-22

Li, R., Xu, H., Tang, H., Shen, J., & Xu, Y. (2023). Characteristics of extended-spectrum β-lactamase–producing *Escherichia coli* in bloodstream infections. *Infection and Drug Resistance, 16*, 2043–2060. https://doi.org/10.2147/IDR.S400170

Liu, B., Talukder, M.J.H., Terhonen, E., Lampela, M., Vasander, H., Sun, H., & Asiegbu, F. (2020). Microbial diversity and structure in peatland forests in Indonesia. *Soil Use and Management, 36*(1), 123–138. https://doi.org/10.1111/sum.12543

Luan, G., & Drlica, K. (2018). Fluoroquinolone–gyrase–DNA cleaved complexes. In *Methods in molecular biology* (pp. 269–281). Springer. https://doi.org/10.1007/978-1-4939-7459-7_19

Mahdiyah, D., Farida, H., Riwanto, I., Mustofa, M., Wahjono, H., Laksana Nugroho, T., & Reki, W. (2020). Screening of Indonesian peat soil bacteria producing antimicrobial compounds. *Saudi Journal of Biological Sciences, 27*(10), 2604–2611. https://doi.org/10.1016/j.sjbs.2020.05.033

Mahdiyah, D., Hidayah, N., Darsono, P.V., & Mukti, B.H. (2025a). Discovery of a novel *Lysinibacillus* species from Indonesian peat soil with potent anti-multidrug-resistant activity. *Pakistan Journal of Biological Sciences, 28*(2), 95–101. https://doi.org/10.3923/pjbs.2025.95.101

Mahdiyah, D., Hidayah, N., Darsono, P.V., & Mukti, B.H. (2025b). Antibiotic compounds from peat *Lysinibacillus banjarense* Mahdiyah. In *Innovating for a sustainable future: Through research, education, and collaboration for planetary well-being* (p. 40).

Mahdiyah, D., Wahyudi, A.T., Widanarni, & Farida, H. (2019). *Jaspis* sp. sponge-associated bacteria producing protease inhibitors. *Pakistan Journal of Medical & Health Sciences, 13*(4), 1245–1252.

Maher, C., & Hassan, K.A. (2023). The Gram-negative permeability barrier: Tipping the balance of the in and the out. *mBio, 14*(6), e01205-23. https://doi.org/10.1128/mbio.01205-23

Manalu, S.P., Sabrina, T., & Sari, Y.A. (2024). Exploring the triad: pH, nitrogen, and phosphorus characteristics of peat soils in Humbang Hasundutan Regency. *E3S Web of Conferences, 519*, 03009. https://doi.org/10.1051/e3sconf/202451903009

Margaryan, A., Panosyan, H., & Birkeland, N.-K. (2021). Heavy metal resistance in prokaryotes: Mechanisms and applications. In *Microbial metal resistance* (pp. 273–313). Springer. https://doi.org/10.1007/978-981-16-3731-5_13

Mishra, R., Kushveer, J.S., Khan, M.I.K., Pagal, S., Meena, C.K., Murali, A., Dhayalan, A., & Venkateswara Sarma, V. (2020). 2,4-Di-tert-butylphenol isolated from an endophytic fungus, *Daldinia eschscholtzii*, reduces virulence and quorum sensing in *Pseudomonas aeruginosa*. *Frontiers in Microbiology, 11*, 1668. https://doi.org/10.3389/fmicb.2020.01668

Mody, H., Kowthavarapu, V.K., & Betts, A. (2025). Recent advances in PK/PD and quantitative systems pharmacology models for biopharmaceuticals. In *Biopharmaceutical informatics* (pp. 307–343). CRC Press. https://doi.org/10.1201/9781003300311-12

Mohamad, H.M., Sulaiman, M.A.H., Saida, N.A., Suhaimi, A.A., Sutarno, M.S., Md Talib, F., Zainorabidin, A., & Suro, S.M. (2024). Klias peat soil: A

depth-based property assessment. *Journal of Soil, Environment & Agroecology, 3*(1), 9–28. https://doi.org/10.37934/sea.3.1.928

Mukti, B.H. (2024). Ethnobotanical studies of medicinal plants in Borneo: Bridging tradition and pharmaceutical research. *Health Sciences International Journal, 2*(2), 154–168. https://doi.org/10.71357/hsij.v2i2.41

Ortiz, A., & Sansinenea, E. (2023). Chemical profiling of metabolites of *Bacillus* species: A case study. In *Rhizobiome* (pp. 445–456). Elsevier. https://doi.org/10.1016/B978-0-443-16030-1.00004-3

Páez-Vélez, C., Rivas, R.E., & Dussán, J. (2019). Enhanced gold biosorption of *Lysinibacillus sphaericus* CBAM5 by encapsulation of bacteria in an alginate matrix. *Metals, 9*(8), 818. https://doi.org/10.3390/met9080818

Pendyukhova, A.S., Belkova, N.L., Okhotina, Y.S., Ivanchikov, E.A., Shchekotova, A.V., Semenova, N.V., & Rychkova, L.V. (2024). Antagonistic activity of monocultures and consortia of lactobacilli against multidrug-resistant opportunistic bacteria as screening of probiotic potential. *Acta Biomedica Scientifica, 9*(3), 121–129. https://doi.org/10.29413/ABS.2024-9.3.12

Pires, D.E.V., Blundell, T.L., & Ascher, D.B. (2015). pkCSM: Predicting small-molecule pharmacokinetic and toxicity properties using graph-based signatures. *Journal of Medicinal Chemistry, 58*(9), 4066–4072. https://doi.org/10.1021/acs.jmedchem.5b00104

Pratiwi, E., Satwika, T.D., & Agus, F. (2021). Analysis of peat bacterial diversity in oil palm plantations and a logged forest in Jambi, Indonesia using PCR-DGGE. *IOP Conference Series: Earth and Environmental Science, 648*(1), 012200. https://doi.org/10.1088/1755-1315/648/1/012200

Prusty, I. (2024). Exploring new avenues in drug discovery and development: Insight into pharmacokinetics and pharmacodynamics. *Journal of Applied Bioanalysis, 10*, 53–55. https://doi.org/10.53555/jab.v10.006

Ranganathan, S., Nagarajan, H., Busi, S., Ampasala, D.R., & Lee, J.-K. (2024). Mechanistic understanding of antibiotic resistance in ESKAPE pathogens. In *ESKAPE pathogens* (pp. 79–118). Springer Nature Singapore. https://doi.org/10.1007/978-981-99-8799-3_3

Rouvier, F., Abou, L., Wafo, E., Andre, P., Cheyrol, J., Khacef, M.-M., Nappez, C., Lepidi, H., & Brunel, J.M. (2024). Identification of 2,4-di-tert-butylphenol as an antimicrobial agent against *Cutibacterium acnes* isolated from Rwandan propolis. *Antibiotics, 13*(11), 1080. https://doi.org/10.3390/antibiotics13111080

Sakalauskienė, G.V., Malcienė, L., Stankevičius, E., & Radzevičienė, A. (2025). Unseen enemy: Mechanisms of multidrug antimicrobial resistance in Gram-negative ESKAPE pathogens. *Antibiotics, 14*(1), 63. https://doi.org/10.3390/antibiotics14010063

Sayed, A.M., Hassan, M.H.A., Alhadrami, H.A., Hassan, H.M., Goodfellow, M., & Rateb, M.E. (2020). Extreme environments: Microbiology leading to specialized metabolites. *Journal of Applied Microbiology, 128*(3), 630–657. https://doi.org/10.1111/jam.14386

Shahanawaz, M., Singh, K., Kushwaha, S.P., Kumar, A., Suvaiv, & Shafiurrahman (2024). Outer membrane permeability enhancers. In *Antimicrobial resistance: Mechanisms and therapeutic strategies* (pp. 148–170). IGI Global. https://doi.org/10.4018/979-8-3693-1540-8.ch006

Sun, J., He, X., Le, Y., Al-Tohamy, R., & Ali, S.S. (2024). Potential applications of extremophilic bacteria in the bioremediation of extreme environments contaminated with heavy metals. *Journal of Environmental Management, 352*, 120081. https://doi.org/10.1016/j.jenvman.2024.120081

Suvidhi, M., Kumar, S., Sumanshu, M., & Vaid, R.K. (2024). *In silico* ADMET predictions: Enhancing drug development through QSAR modeling. In *Futuristic trends in agriculture engineering & food sciences* (Vol. 3, Book 21, pp. 41–52). Iterative International Publisher. https://doi.org/10.58532/V3BCAG21P2CH1

Trott, O., & Olson, A.J. (2010). AutoDock Vina: Improving the speed and accuracy of docking with a new scoring function, efficient optimization, and multithreading. *Journal of Computational Chemistry, 31*(2), 455–461. https://doi.org/10.1002/jcc.21334

Vaara, M. (2020). Lipopolysaccharide and the permeability of the bacterial outer membrane. In *Endotoxin in health and disease* (pp. 31–38). CRC Press. https://doi.org/10.1201/9781003064961-2

Velusamy, P., Jeyanthi, V., Pachaiappan, R., Anbu, P., & Gopinath, S.C.B. (2024). Secretion of 2,4-di-tert-butylphenol by a new *Pseudomonas* strain SBMCH11: A tert-butyl substituted phenolic compound displaying antibacterial efficacy. *Results in Chemistry, 8*, 101593. https://doi.org/10.1016/j.rechem.2024.101593

Vergalli, J., Atzori, A., Pajovic, J., Dumont, E., Malloci, G., Masi, M., Vargiu, A. V., Winterhalter, M., Réfrégiers, M., Ruggerone, P., & Pagès, J.-M. (2020). The challenge of intracellular antibiotic accumulation: A function of fluoroquinolone influx versus bacterial efflux. *Communications Biology, 3*(1), 198. https://doi.org/10.1038/s42003-020-0929-x

Wang, W., Melnikov, F., Napoli, J., & Desai, P. (2024). Advances in the application of *in silico* ADMET models: An industry perspective. In *Computational drug discovery* (pp. 495–535). https://doi.org/10.1002/9783527840748.ch21

World Health Organization (WHO) (2025). *Global antibiotic resistance surveillance report 2025: WHO Global Antimicrobial Resistance and Use Surveillance System (GLASS)*. WHO.

Wulandari, W., Purwaningsih, Y., & Syukur, M. (2022). Potensi antibakteri sintesis mentil sinamat terhadap bakteri *Staphylococcus aureus*, methicillin-resistant *Staphylococcus aureus*, *Escherichia coli*, dan *Salmonella Typhi*. *Cendekia Eksakta, 7*(1), 65–51. https://doi.org/10.31942/ce.v7i1.6551

Yang, L., Wang, R., Lin, W., Li, B., Jin, T., Weng, Q., Zhang, M., & Liu, P. (2024). Efficacy of 2,4-di-tert-butylphenol in reducing *Ralstonia solanacearum* virulence: Insights into the underlying mechanisms. *ACS Omega, 9*(4), 4647–4655. https://doi.org/10.1021/acsomega.3c07887